Journal of Physics: Conference Series **274** (2011) 012022 doi:10.1088/1742-6596/274/1/012022

Optically coupled cavities for wavelength switching

Pablo A. Costazo-Caso[1,2], Sergio Granieri[1], and Azad Siahmakoun[1]

[1] Department of Physics and Optical Engineering, Rose-Hulman Institute of Technology, 5500 Wabash Avenue, Terre Haute, IN 47803 (United States)
[2] Centro de Investigaciones Ópticas (CONICET La Plata-CIC) and Facultad de Ingeniería Universidad Nacional de La Plata. Camino Centenario y 506, La Plata 1900 (Argentina)

E-mail: pcostanzo@ing.unlp.edu.ar, granieri@rose-hulman.edu, siahmako@rose-hulman.edu

Abstract. An optical bistable device which presents hysteresis behavior is proposed and experimentally demonstrated. The system finds applications in wavelength switching, pulse reshaping and optical bistability. It is based on two optically coupled cavities named master and slave. Each cavity includes a semiconductor optical amplifier (SOA), acting as the gain medium of the laser, and two pair of fiber Bragg gratings (FBG) which define the lasing wavelength (being different in each cavity). Finally, a variable optical coupler (VOC) is employed to couple both cavities. Experimental characterization of the system performance is made analyzing the effects of the coupling coefficient between the two cavities and the driving current in each SOA. The properties of the hysteretic bistable curve and switching can be controlled by adjusting these parameters and the loss in the cavities. By selecting the output wavelength (λ_1 or λ_2) with an external filter it is possible to choose either the invert or non-invert switched signal. Experiments were developed employing both optical discrete components and a photonic integrated circuit. They show that for 8 m-long cavities the maximum switching frequency is about 500 KHz, and for 4 m-long cavities a minimum rise-time about 21 ns was measured. The switching time can be reduced by shortening the cavity lengths and using photonic integrated circuits.

Acronyms

CW: Continuous wave laser
EDFA: Erbium-doped fiber amplifier
EOM: Electro-optic modulator
FBG: Fiber Bragg grating
FIL: Optical filter
FP: Fabry-Perot
MZI: Mach-Zehnder interferometer
OSA: Optical spectrum analyzer
OSC: Oscilloscope
PC: Polarization Controler
PD: Photodiode
SOA: Semiconductor optical amplifier
VOA: Variable optical attenuator
VOC: Variable optical coupler

1. Introduction

Photonic routing and processing to solve the problem of growth in demand for transmission capacity in future network, continues attracting the attention of the scientific community and researchers. Monolithic and hybrid photonic integration have lined up to provide the enabling technology to design the next generation of photonic networks and devices [1]. All-optic bistable devices are studied connected to different applications and complex systems as wavelength converters, wavelength routers, optical flip-flops, neural networks and pulse shapers. They have been demonstrated employing hybrid optoelectronic systems [2-3]. In a previous work [4], two coupled fiber ring resonators were proposed for optical neural network and flip-flop applications. The main disadvantage of this component is that requires optical isolators and then is not suitable for all optical integration.

In this paper, it is presented a photonic device to produces optical bistability, wavelength conversion and pulse reshaping based-on two coupled Fabry-Perot (FP) cavities which do not require optical isolators. The device has a different configuration from the proposed in [5] and also here it is employed a photonic integrated circuit which include the amplifiers and couplers. The device is developed and experimentally characterized. It can produce two different wavelengths at the output, one inverted and the other not, which can be chosen by properly adjusting the filter wavelength. Depending on the pump powers (injection currents) and the input power, the resulting output is a reshaped signal of the corresponding input.

2. Principle of operation and experiments

The The coupled lasers here considered consist of two optically coupled Fabry-Perot cavities which we named master and slave because one of them is set to have a dominant emission. Each cavity includes a semiconductor optical amplifier (SOA), actuating as gain medium of the laser, and two fiber Bragg gratings (FBG) which define the lasing wavelength (being different for each cavity). Finally, an optical coupler is employed to couple both cavities as is shown at the top of Figure 1. The device operates on the basis of the non linear effect known as gain quenching in the SOAs. Therefore, if the master laser (laser 2) is lasing at λ_2 it reduces the gain in the slave cavity (laser 1) quenching its emission at λ_1. In this state, the output power is high at λ_2 and low at λ_1. When the master laser is turned off, the gain of the slave laser increases and starts to lase. At this point, the output power is high at λ_1 and low at λ_2. The master laser is controlled with and external laser operating at a different wavelength λ_3.

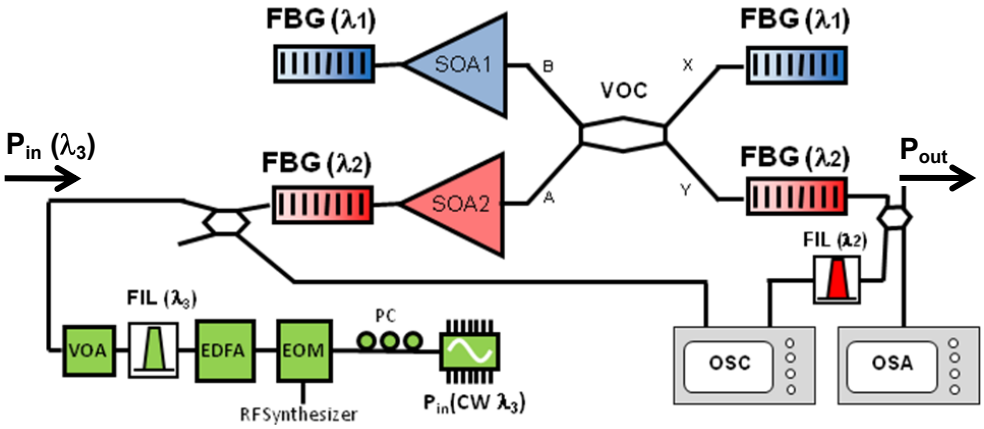

Figure 1. Experimental setup employing discrete components to produces optical bistability in the FP coupled cavities.

For obtaining laser emission in the nth cavity the gain G_n of the corresponding SOA must compensate for any loss in the cavity (expressed by T_{nn} in equation (1a)). The nature of the emission during the transition from laser 2 to laser 1, depends on the relationship between the transmittance of each cavity and the cross transmittance between them. We define the own transmittance of the nth cavity, T_{nn}, and the cross transmittance from nth cavity to mth cavity, T_{nm}, as

$$T_{nn} = R_{nL} R_{nR} K_{nn} \alpha_{nn} \tag{1a}$$

$$T_{nm} = R_{nL} R_{nR} K_{nm} \alpha_{nm} \tag{1b}$$

where α_n is the fiber loss of the nth cavity, R_{nL} and R_{nR} are the left and right FBG reflectivities and K_{nn} and K_{nm} are the direct and cross coupling ratio (n, m = 1, 2). Three different cases can be considered: $T_{nn} < T_{nm}$, $T_{nn} > T_{nm}$ and $T_{nn} = T_{nm}$. The first case produces a certain amount of hysteresis in the transition between the two states (this mean that the output can takes two different values for the same input, depending on the previous operation condition), whereas the last two cases present a few differences in the transition but hysteresis is not observed. [4]

2.1. Optical bistable switch

An optical system implemented with discrete components is used to produce a bistable device with hysteresis behavior. Figure 1 shows the developed coupled cavities with two Covega SOAs, two pairs of FBGs centered at wavelengths λ_1 = 1551.69 nm and λ_2 = 1553.5 nm which are employed as mirrors and filters of each FP cavity, and a VOC to couple both cavities. The external laser is modulated by an electro-optic modulator (EOM) and introduced to the master laser to control the transition. The input power is adjusted through an erbium doped fiber amplifier (EDFA) and a variable optical attenuator (VOA). A tunable optical filter (FIL) is used to select the power at λ_3 cancelling the amplified spontaneous emission of the EDFA. By adjusting a tunable filter, the output signal can be measured either at the wavelength of the master laser, λ_2, or the slave laser, λ_1, depending if the inverted or non inverted output is required.

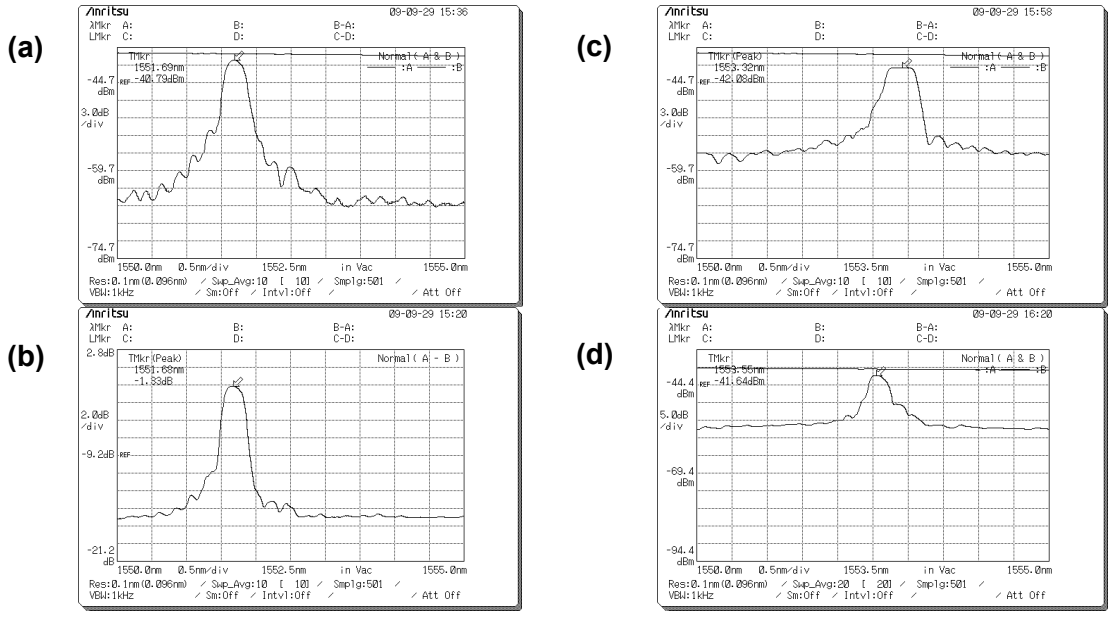

Figure 2. Measured reflection spectrum for the four FBGs. (a) and (b) FBGs are centered at the wavelength 1551.6 nm and (c) and (d) at the wavelength 1553.5 nm.

Because a hysteretic bistable device requires that the condition $T_{nn} < T_{nm}$ be satisfied, the coupling coefficient in the VOC is properly adjusted to produce this asymmetry. The reflection spectrums of the four FBGs are shown in Figures 2(a) and (b), for λ_1; and (c) and (d), for λ_2. The bandwidths of the gratings are in the range 0.4-0.6 nm and the reflectivities are given by: $R_{1L} = 0.41$; $R_{1R} = 0.66$; $R_{2L} = 0.55$ and $R_{2R} = 0.49$ (calculated from the measured insertion loss: 3.91 dB; 1.83 dB; 2.62 dB and 3.06 dB, respectively). Therefore, by considering that the loss α in both cavities are same, the condition $T_{22} < T_{21}$ is easily satisfied by selecting the coupling coefficient around 60/40. The master and slave cavities have threshold currents about 180 mA. Consequently, the injection current supplied to the SOAs are set as $I_{SOA1} = 190$ mA and $I_{SOA2} = 250$ mA in order that cavity 2 be dominant and quenches cavity 1. External light at wavelength $\lambda_3 = 1552.8$ nm is injected into master laser via the corresponding FBG_2. The injected power, 15 dBm, is controlled by the EDFA which is fixed as the required power to turn off the master laser. By using the VOA located at the external laser path, it is possible to turn on and off the input power to the cavity 2 via the VOA's shutter. Therefore, when the shutter is OFF, the power gets in to the master cavity quenching the gain of the SOA_2 producing that the laser 1 starts to lase. Otherwise, when the shutter is ON, the input power is close to zero, laser 2 is lasing and quenches the slave cavity. Figure 3 shows the measured optical spectrum in both conditions: (a) shutter is OFF and the output power is at wavelengths λ_1 and λ_3, and (b) shutter is ON and the output power is at wavelength λ_2.

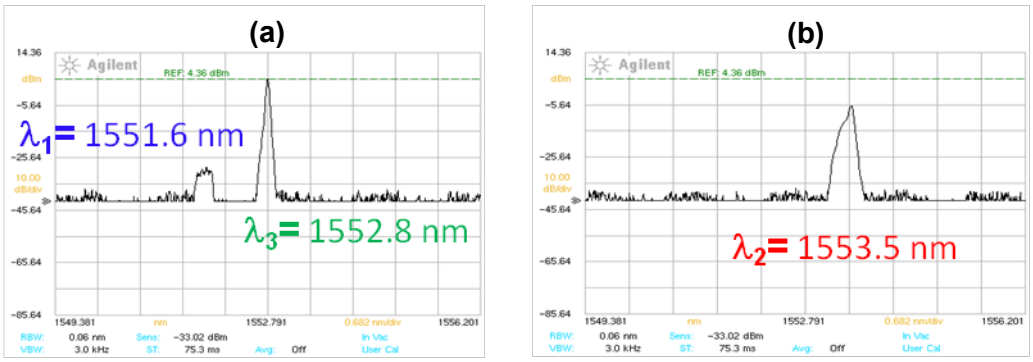

Figure 3. Optical spectrum when the attenuator shutter is: (a) OFF being the optical peak power $P_{\lambda 1}$ = -28 dBm and $P_{\lambda 3}$ = 4.3 dBm; and (b) ON being $P_{\lambda 2}$ = -5.5 dBm.

Finally, in order to demonstrate the input-output characteristic curve and the frequency response of the system, the external laser is modulated by a Lucent 20 GHz bandwidth EOM, which is fed with a sinusoidal signal as shown in Figure 1. The parameters of the cavities are remained as in the spectrum measurements (SOA driving currents, coupling coefficient, etc) as well as the input power of the external laser. The cavity length is about 6 m-long which defines a round-trip-time of 30 ns. This time represent the theoretical limit for the rise/fall time of the output. However, because the system includes two coupled cavities the temporal response is much larger. Figures 4(a)-(c) show the measured signals in the oscilloscope for three different frequencies 100, 200 and 500 KHz, respectively. The upper trace show the detected input signal at wavelength λ_3, the middle trace the detected output signal at λ_2, and the bottom trace show the hysteresis curve obtained as the input vs. output signals. The resulting rise- and fall-time are 500 ns and 1.5 us for 100 KHz. Notice that when the external laser power goes down, laser 2 is turned on and the rise time is faster. However, the output power continues growing up and no saturation is observed at the output signal. In the other side, when the external laser power goes up, laser 2 takes more time to be turned off although the output reaches the saturation region. While the rise-time is constant for all the frequencies, the fall-time increases as

the frequency increases. It can be seen in the bistable curves as a left-side transition is moving to the left as the frequency is increased. The effect produced by changing the injection current of the SOAs (or the gain of the cavities) is to modify the threshold values of the hysteresis loop moving the shape. If the SOA_2 current is increased (or SOA1 current is decreased) the hysteresis loop is moving toward to right. Otherwise, the hysteresis loop is shifted to the left.

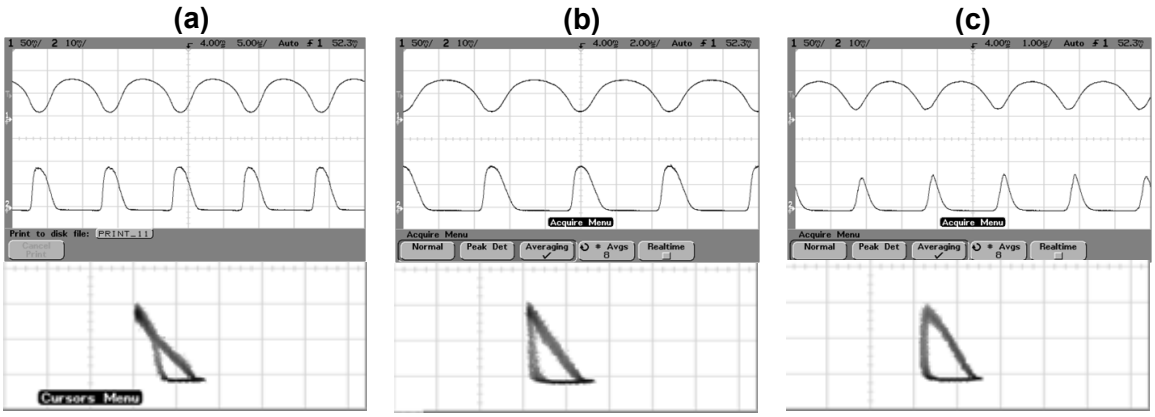

Figure 4. Input signal (upper trace) bistable output (middle trace) and hysteretic bistable curve obtained from the input and output signals (bottom trace) for: (a) 100 KHz; (b) 200 KHz and (c) 500 KHz input frequencies.

2.2. Wavelength switching and pulse reshaping

The coupled cavities also were implemented with an integrated SOA-based Mach-Zehnder interferometer (SOA-MZI) which is provided by the CIP company. The system is depicted in Figure 5 and it is used to provide wavelength switching and pulse reshaping. All couplers inside the SOA-MZI are 50:50. It means the relation $T_{nn} = T_{nm}$ is satisfied for similar FBG reflectivities and attenuation (as it was demonstrated by equations (1)). Two pairs of FBGs at wavelengths $\lambda_1 = 1549.8$ nm and $\lambda_2 = 1555.6$ nm were employed as mirrors and filters in each Fabry-Perot cavity. The used FBGs have a similar bandwidth, about 0.5 nm, and the reflection insertion loss is approximately 1.2 dB. The cavity lengths are 4 m due to the fiber connections of the CIP device and the FBGs. The external input comes from a Santec tunable laser at the wavelength $\lambda_3 = 1559.8$ nm. This laser is modulated with an EOM, amplified by an IPG Photonics EDFA and properly filtered. Finally, a variable attenuator and a 10/90 coupler are employed to monitor and control the input power to the system. The slave cavity operating at λ_1 has a threshold current of 70 mA, an injection current (driving the SOA_1) of $I_{SOA1} = 80$ mA, and the resulting output power is $P_1 = -15.4$ dBm. The master cavity operating at λ_2 has a threshold current of 60 mA, the injection current (driving the SOA_2) is $I_{SOA2} = 80$ mA, and the output power is $P_2 = -8.6$ dBm. The SOA currents were set asymmetrically in order that one laser works as a dominant (master) quenching the slave laser when the input power is zero.

Figure 6(a) shows the output power measured with an Agilent optical spectrum analyzer (OSA) at λ_1 and λ_2, as a function of the input power at λ_3. It is possible to see how the output power of the master laser decreases with the input power having a characteristic slope that depends on the losses of the cavity. Moreover, the slave laser begins to lase when the gain exceeds the losses. The output power increases with input power showing a different slope which is characteristic of this cavity. It takes place until it reaches the saturation power. Figures 6(b) and (c) show the measured output spectra for input powers -24 dBm and 3.5 dBm respectively. The corresponding output powers are: $P_1 = -8.5$ dBm and $P_2 = -36.8$ dBm, for the former, and $P_1 = -33.8$ dBm and $P_2 = -13.07$ dBm, for the latter. The

contrast ratio for both states is between 18 and 20 dB. It can be observed how by controlling the power of the external laser, the wavelength of the output signal is chosen.

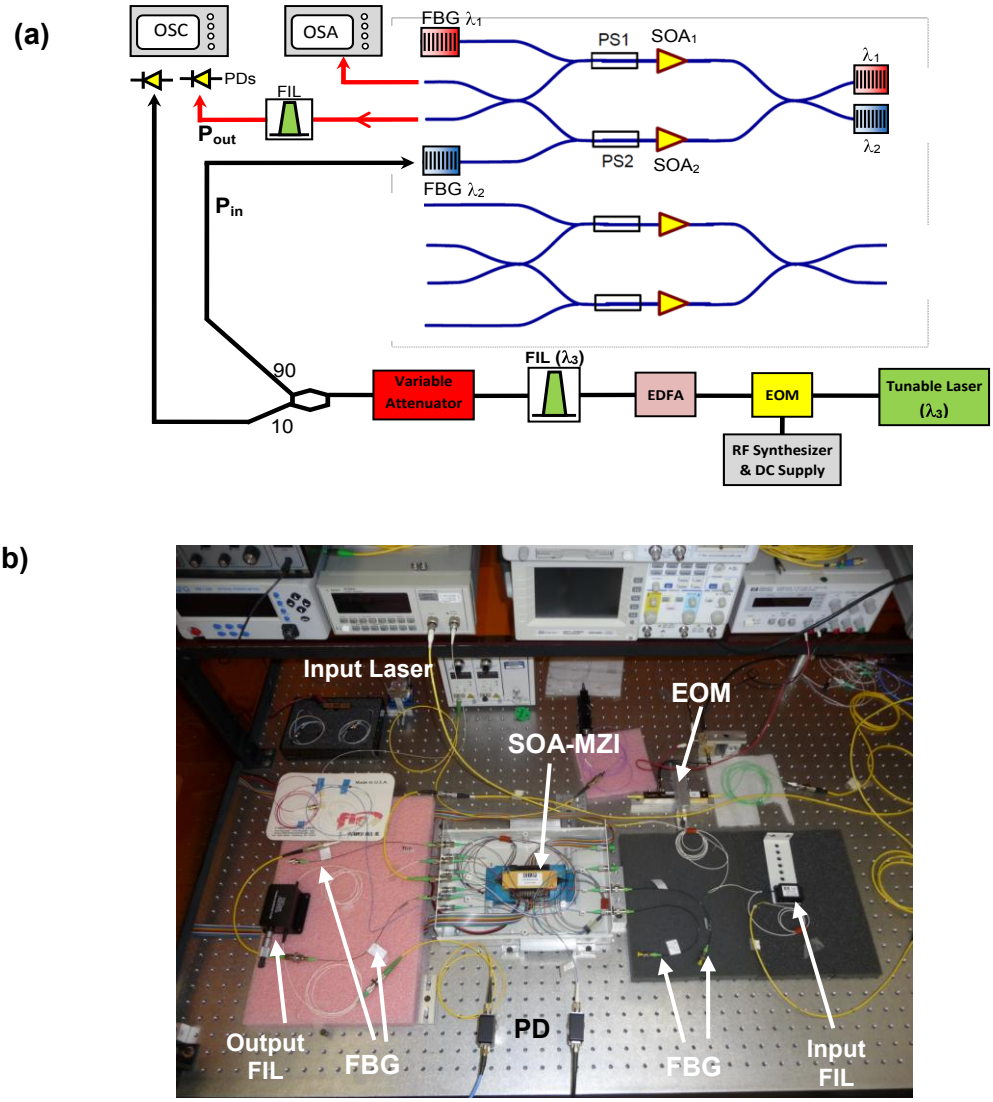

Figure 5. (a) Experimental setup employing the top section of the CIP integrated device. Two pairs of FBG at λ_1 and λ_2 form the cavities and define the output emission wavelengths. (b) Corresponding picture token in the laboratory.

Now, let us consider that a modulated signal, consisting of spread pulses, is introduced at the input of the system. The device can reshape the waveform generating pulses with more abrupt edges and in two different output wavelengths. Experiments show that the rising time is mainly depending of the cavity lengths and the length between the two SOAs, while the falling time also is dependent of the input signal [6]. In our systems the cavity lengths is approximately 4 m-long which represent a round-trip-time of 20 ns, being this value the theoretical limit for the rise/fall times. Figure 5 shows the experimental setup where a sinusoidal signal is employed to modulate the input laser at λ_3. The output signal is filtered in a Dicon tunable filter (to choose the required wavelengths λ_1 or λ_2), detected in a Thorlabs 1 GHz bandwidth photodetector, and measured in an Agilent digital scope.

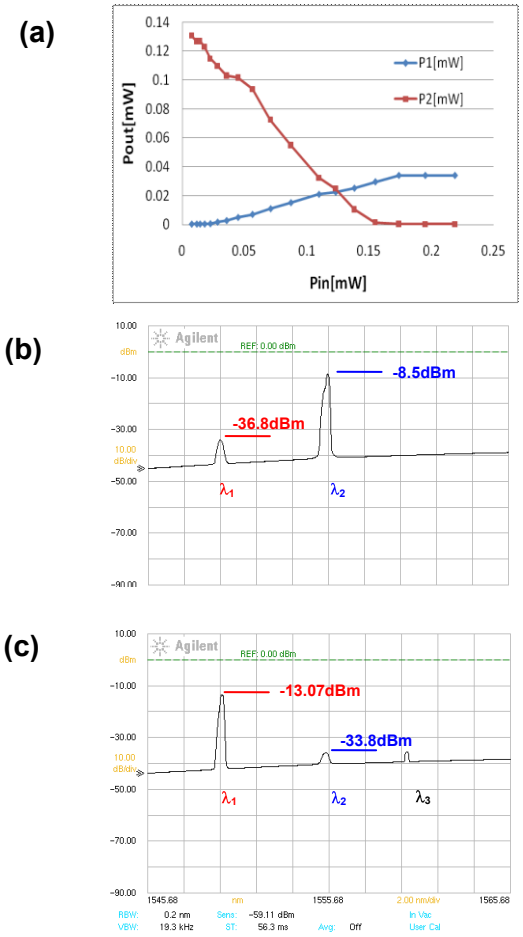

Figure 6. (a) Measured output powers at λ_1 and λ_2 as a function of the input power at λ_3. Spectra of the output signal for input powers equal to powers -24 dBm (b); and 3.5 dBm (c).

Figures 7(a)-(d) show the responses of the device for several input sinusoidal signals having different frequencies. In the top side of each figure it is illustrated the input signal and in the botton side the detected output signal. Figures 7(a) and (b) show the outputs at λ_1 and at λ_2 respectively, for a 10 KHz input frequency. The output signals have a good resemblance with a square wave, although for the signal at wavelength λ_1 the high level of the pulses presents some distortion. Figures 7(c) shows the output at λ_1 for an input frequency of 1 MHz; while (d) shows the output at λ_2, for an input frequency of 10 MHz. Despite the output signals do not have a square waveform, it is evident the improvement with respect to the sinusoidal input. The measured edge times are 140 ns in the first case and 26 ns in the second case.

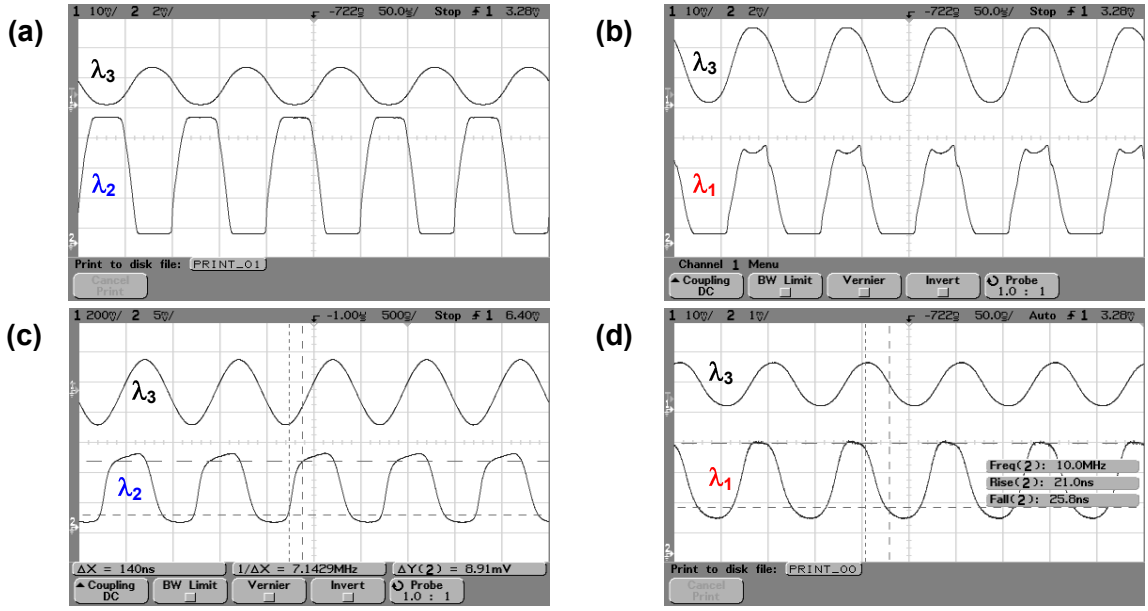

Figure 7. Detected input modulated signals (top of each figure) and detected outputs at wavelength λ_1 or λ_2 (bottom of each figure), for different frequencies: (a) 10 KHz at λ_2; (b) 10 KHz at λ_1; (c) 1 MHz at λ_2; and (b) 10 MHz at λ_1. The minimum rise and fall are 21 ns and 26 ns respectively.

3. Conclusions

We have analyzed and characterized two Fabry-Perot coupled cavities that exhibit bistability and hysteresis behavior. The discrete-based components prototype is used to demonstrate switching between to stable states at different frequencies. The switching thresholds and the shape of the hysteresis loop can be controlled by properly choosing the SOA currents as well as the coupling ratio between the cavities. Improvements in the response time of the system can be achieved by decreasing the length of the cavities (because the photon life time of the cavity decreases) and improving the extinction ratio of the modulated input signal.

Then, the two coupled Fabry-Perot cavities were built in an integrated SOA-MZI device together with two pairs of external FBGs. It was employed for wavelength conversion and pulse reshaping applications. The resultant contrast ratio between the two output wavelengths about 20 dB is a suitable value for most applications requiring optical switching and wavelength routing. In addition, a pulse re-shaper was demonstrated at two different wavelengths. The minimum rise/fall times is in tens ns range limited mainly for the length of the cavities (about 4 m-long).

Acknowledgments

This work was partially supported by Indiana RF Alliance, Polyphase Microwave Inc, TSC and NSWC-Crane Division, Crane, IN. Pablo A. Costanzo Caso acknowledges the support of CONICET (PIP 112-200801-01769), Facultad de Ingeniería Universidad Nacional de La Plata (Project I128) and ANPCyT (PICT 0378/08 and 38289/05).

References

[1] Stampoulidis L, Petrantonakis D, Stamatiadis C, Kehayas E, Bakopoulos P, Kouloumentas C, Zakynthinos P, Vyrsokinos K, Dekker R and Klein E J Microring-resonator-assisted, all-optical wavelength conversion using a single SOA and a second-order Si3N4–SiO2 ROADM 2010 *IEEE J. Lightw. Technol.* **28** 476-83

[2] Liu Y *et al*. Ultrafast all-optical wavelength routing of data packets utilizing an SOA-based wavelength converter and a monolithically integrated optical flip–flop 2008 *IEEE J. Sel. Topics Quantum Electron.* **14** 801-7
[3] Clavero R, Ramos F and Marti J All-optical flip-flop based on an active Mach–Zehnder interferometer with a feedback loop 2005 *OSA Opt. Lett.,* **30**, 2861-3
[4] Hill M T, Frietman E E, de Waardt H, Khoe G D and Dorren H J S All fiber-optic neural network using coupled SOA based ring lasers 2002 *IEEE Transactions on Neural Networks* **13** 1504-13
[5] Hill M T, de Waardt H, Khoe G D and Dorren H J S All-optical flip-flop based on coupled laser diodes 2001 *IEEE J. Quantum Electron.* **37** 405-13
[6] Malacarne A, Wang J, Zhang Y, Das Barman A, Berrettini G, Poti L and Bogoni A 20 ps transition time all-optical SOA-based flip-flop used for photonic 10 Gb/s switching operation without any bit loss 2008 *IEEE J. Sel. Topics Quantum Electron.* **14** 808-15